Available online at www.sciencedirect.com
ScienceDirect
Ceramics International 38 (2012) 769–774
CERAMICS INTERNATIONAL
www.elsevier.com/locate/ceramint

Densification behavior and microstructure of spark plasma sintered ZrB_2-based composites with SiC particles

Masahide Ikegami [a], Shuqi Guo [b,*], Yutaka Kagawa [a,b]

[a] Research Center for Advanced Science and Technology, The University of Tokyo, 4-6-1 Komaba, Meguro-ku, Tokyo 153-8505, Japan
[b] Hybrid Materials Unit, National Institute for Materials Science, 1-2-1 Sengen, Tsukuba, Ibaraki 305-0047, Japan

Received 27 April 2011; received in revised form 28 June 2011; accepted 1 August 2011
Available online 27th August 2011

Abstract

The densification behavior and microstructure of spark plasma sintered ZrB_2-based composites with SiC particles were examined. The effects of the amount and size of the SiC particles added were assessed. The results indicated that sinterability of the composites was improved by the addition of SiC compared with single-phase ZrB_2 ceramics. This improvement depended on the effects of the amount and size of SiC particles added. Relative densities exceeding 98% were obtained for ZrB_2–SiC powders sintered at 1900 °C for 2 min under a pressure of 30 MPa. The microstructure of the resulting composites was fine and homogeneous, and the average grain size of ZrB_2 decreased with increase in the amount of SiC and with decrease in SiC particle size.

Keywords: ZrB_2; Densification; Microstructure; Spark plasma sintering

1. Introduction

High-temperature stability and thermo-mechanical performance of ZrB_2 ultra-high temperature ceramics have recently been receiving particular attention because they are expected to be used as heat-resist components in near future [1–5]. However, it is acknowledged that ZrB_2 has poor sinterability and that sintering aids are needed to obtain a fully dense bulk material. To improve sinterability of ZrB_2, various nitrides, carbides, silicides, and metals, such as SiC [3,5–9], AlN [10], B_4C [11], Cu [12], $MoSi_2$ [8], and $ZrSi_2$ [13], have been used as aids. Among these sintering aids, SiC has proved to be one of the most effective. In addition, the addition of SiC contributes to improvement of oxidation resistance of ZrB_2 ceramics as the result of formation of glassy protective layers in high-temperature oxidation environments [3,14].

Recently, nearly fully dense ZrB_2-based composites with SiC have been consolidated by hot pressing [3,6,7,9] and spark plasma sintering (SPS) [8,15]. Advantages of the SPS process are short sintering time and rapid heating rate compared with the conventional hot pressing process [16–18], thus allowing a fine and homogeneous microstructure of the resulting materials to be maintained. On the other hand, it is known that powder size and composition are important factors that affect the densification behavior and microstructure of sintered materials. However, the effects of the amount and size of the added SiC particles on the densification behavior of ZrB_2-based composites with SiC are little known. Therefore, in order to obtain fully dense composites with fine and homogeneous microstructure it is first necessary to ascertain the effects of the amount and size of added SiC particles on the densification behavior and microstructure of the composites.

This study focuses on an examination of the densification behavior and microstructure of ZrB_2-based composites with SiC consolidated by SPS. In addition, the effects of the amount and size of the SiC particles added are examined.

2. Experimental procedure

The starting ZrB_2 powder used in this study had an average particle size of 2.12 μm and was obtained from Japan New Metal (Grade F, Osaka, Japan). To examine the effect of SiC particle size on sinterability of SiC-containing ZrB_2 composites, two starting SiC powders with different particle sizes

* Corresponding author. Tel.: +81 0 29 859 2223; fax: +81 0 29 859 2401.
E-mail address: GUO.Shuqi@nims.go.jp (S. Guo).

0272-8842/$36.00
doi:10.1016/j.ceramint.2011.08.003

were used: powder (A), α-SiC powder (Grade UF-15, H. C. Starck, Berlin, Germany) with an average particle size of 0.5 μm; and powder (B), α-SiC powder (GC #2000, Showa Denko, Tokyo, Japan) with an average particle size of 6.4 μm. Fig. 1 shows scanning electron microscopy (SEM) images of the morphologies of the as-received ZrB_2 and SiC powders. The powder morphologies differed: ZrB_2 had large, round particles; SiC(A) had small, irregularly shaped particles; and SiC(B) had large, angular particles. The amount of SiC added, f_p, was 9, 17, and 23 vol.%, which were determined by knowing the weight ratio of the powders prior to mixing, based on densities of 6.09 and 3.22 g/cm^3 for ZrB_2 and SiC [3], respectively. The powder mixtures were wet mixed using a SiC milling media and ethanol for 24 h, and then dried using an electric resistance heater. Before sintering, the dried mixtures were sieved through a metallic sieve with a 60-mesh screen.

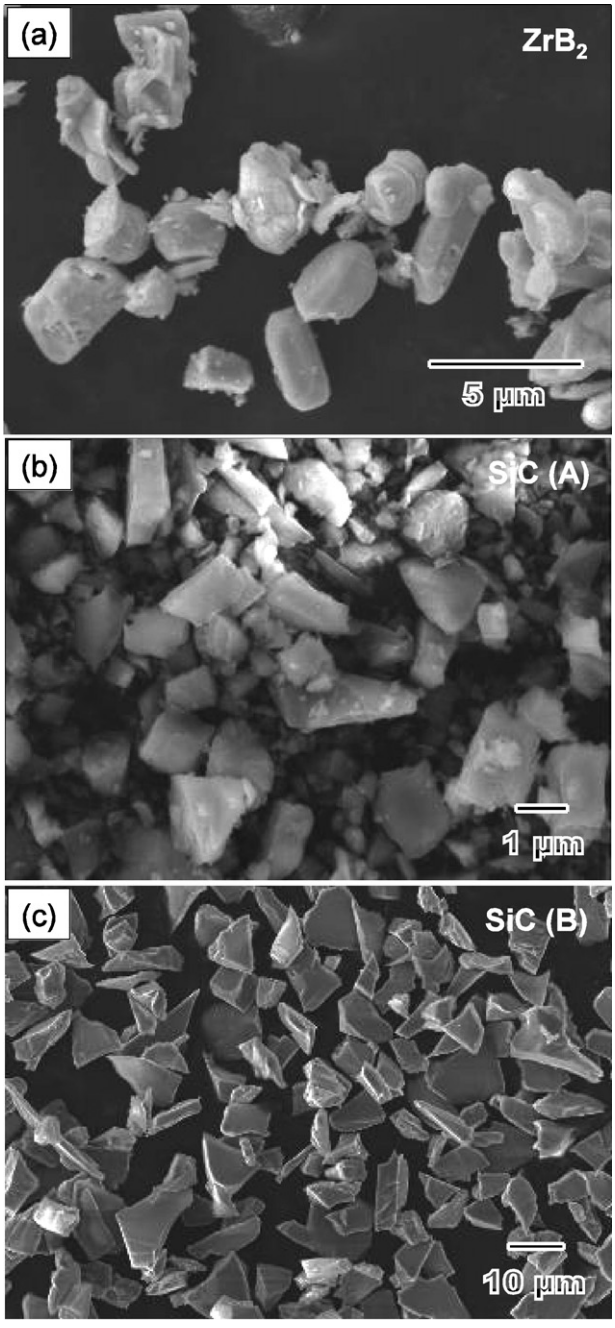

Fig. 1. SEM images of morphologies of as-received powders of (a) ZrB_2, (b) SiC(A), and (c) SiC (B).

A Dr. Sinter SPS-1030 apparatus (Sumitomo Coal Mining Co. Ltd., Tokyo, Japan) was used in this study. The dried ZrB_2–SiC powder mixtures were loaded into a graphite die lined with graphite foil, which has an inner diameter of 15 mm. SPS was conducted at 1900 °C for 2 min in an argon atmosphere with a heating rate of ∼430 °C/min. An uniaxial pressure of 30 MPa was maintained during the SPS cycle. The changes in temperature, T, and sintering displacement, δ_c, during the SPS cycle were recorded by a computer. The final sintered specimens were pellets measuring 15 mm in diameter with a thickness of ∼3 mm.

The densities of the composites were evaluated by the Archimedes method with ethyl alcohol as a medium after removing the surface of the sintered compact to avoid contamination from the graphite die. The theoretical densities of the composites were calculated according to the rule of mixtures. X-ray diffraction was used to identify the crystalline phase presented in the composites using Cu-Kα radiation with a scanning rate of 0.03°/s. The microstructure of the composites was observed by SEM. The grain size of the sintered ZrB_2, d_{ZrB_2}, was determined from SEM images. The grain size, d_{ZrB_2}, was obtained from the measured grain area with circle approximation. The average grain size of ZrB_2, $\bar{d}_{ZrB_2}$, was determined by counting a minimum of 100 grains.

3. Results and discussion

The densification behavior of ZrB_2-based composites with various SiC content was monitored using the sintering temperature–time and displacement–time curves, typical examples of which are shown in Fig. 2. Here δ_c, t, and $d\delta_c/dt$ are displacement, time, and differential of displacement with respect to time during the SPS cycle, respectively. The

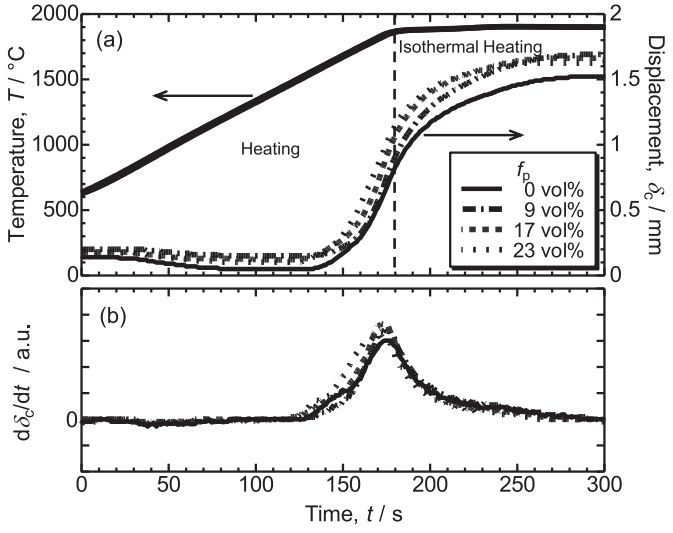

Fig. 2. Effects of SiC content on densification behavior of ZrB_2-based composites with SiC(A); (a) shrinkage curves and (b) shrinkage rate.

beginning of shrinkage was observed at temperatures ranging from 1545 °C to 1570 °C, depending on the amount of SiC added (Fig. 2(a)). The onset temperature of densification was determined to be 1570 °C for single-phase ZrB_2 powder, 1560 °C for 9 and 17 vol.% SiC content, and 1545 °C for 23 vol.% SiC-containing ZrB_2 composites. It was evident that the onset temperature of densification was lower for SiC-containing ZrB_2 ceramics than for single-phase ZrB_2. In particular, for 23 vol.% SiC-containing ZrB_2 composites, the onset temperature of densification was significantly lowered. During subsequent heating, the shrinking rate was significantly dependent on the SiC content, and it increased with increasing amount of SiC added. This indicated that the addition of SiC led to more rapid shrinkage during the SPS cycle compared to single-phase ZrB_2. However, the densification was not completed during the heating and it carried out continuously within a period of ~1 min followed isothermal heating, and then the shrinkage stopped (Fig. 2(a)). The main part of densification occurred within ~2 min, which was much shorter period than with the conventional hot pressing process [19]. The shrinkage rate, $d\delta_c/dt$, changed with time during the SPS cycle, as shown in Fig. 2(b). Each curve represents a different amount of SiC added, and the curves exhibit a peak just before the shrinkage rate decrease. The peak value depended on the SiC content, and it increased with increase in SiC. Thus, addition of SiC promoted densification of ZrB_2-based composites with SiC compared with single-phase ZrB_2, which is a result of higher shrinkage rate.

It is well-known that densification of a single-phase ZrB_2 powder generally requires extremely high temperatures (>2100 °C) [20] owing to the covalent character of the bonding and the low volume and grain boundary diffusion rates [21]. In addition, the presence of B_2O_3 on the surface of the starting powders inhibited densification in non-oxide ceramic systems such as ZrB_2 and TiB_2 because of evaporation of B_2O_3 [21,22]. Therefore, to improve sinterability of ZrB_2, it is necessary to enhance the diffusion rate and reduce the oxygen content, or prevent evaporation of B_2O_3. Improvement of densification due to addition of SiC is documented in the literature. Hwang et al. [6] showed that sinterability of ZrB_2 improved by increasing the amount of SiC added, and highly dense (relative density >97%) ZrB_2-based composites with 22.4 vol.% SiC, with a starting particle size ranging 40 nm–1.7 μm, were hot pressed at 1650 °C under a pressure of 60 MPa with a holding time of 2 h. High-resolution transmission electron microscopy observations showed the presence of the amorphous films in most of the interphase interfaces. Hwang et al. [6] concluded that the improvement in densification due to the addition of SiC is a result of the presence of an intergranular amorphous film. Apparently, the presence of SiO_2 prevents evaporation of B_2O_3 during hot pressing and results in formation of a stable liquid phase among the grains, therefore improving sinterability. It is common for B_2O_3 and SiO_2 films to be present on the surfaces of the starting ZrB_2 and SiC powder particles, respectively. According to the phase diagram for B_2O_3–SiO_2 [23], a stable Si–B–O liquid phase is formed among the grains when B_2O_3 and SiO_2 coexist.

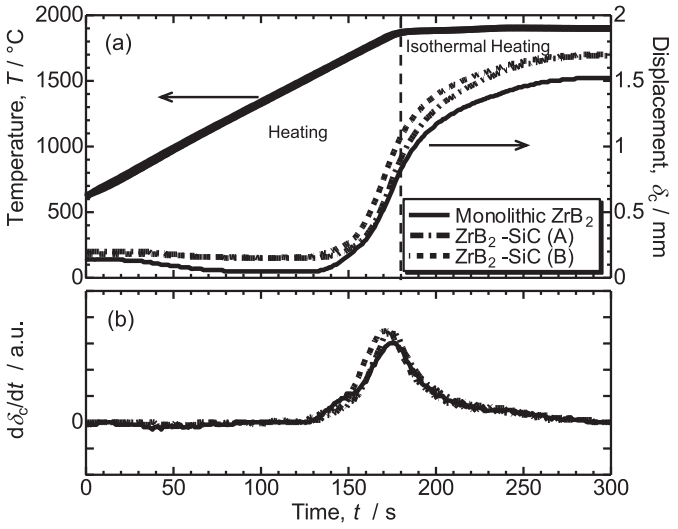

Fig. 3. Effects of particle size of starting SiC powders on densification behavior of ZrB_2-based composites with SiC; (a) shrinkage curves and (b) shrinkage rate (f_p = 9 vol.%).

Thus, a similar intergranular liquid phase is expected for the ZrB_2-based composites with SiC particles investigated in this study. The presence of an intergranular liquid phase favors the process of grain rearrangement and improves the packing density of particles, therefore improving densification. In addition, the amount of the intergranular liquid phase increases with increasing SiC content. Therefore, the shrinkage rate increases and the temperature corresponding to the maximum peak rate decreases with increasing SiC amount.

Fig. 3 shows the effect of size of the starting SiC particles on the shrinkage behavior of ZrB_2-based composites with SiC. It shows that the onset temperature of densification is almost the same for both ZrB_2-9 vol.% SiC(A) (1560 °C) and ZrB_2-9 vol.% SiC(B) (1565 °C), regardless of the size of the starting SiC particles (Fig. 3(a)). However, the ZrB_2-9 vol.% SiC(B) composite showed more rapid shrinkage than the ZrB_2-9 vol.% SiC(A) composite during heating (Fig. 3(b)). Furthermore, a peak shrinkage rate is observed, and the shrinkage is more rapid for the former than for the latter. The densification of both composition powders was completed within a period of ~1 min followed isothermal heating (Fig. 3(a)). Plots of temperature corresponding to the peak shrinkage rate as a function of the amount of SiC added for both ZrB_2-based composites with SiC are shown in Fig. 4. The plots indicate experimental value, and the polygonal lines were derived from average values. The densification curves of those closest to the average are shown in Figs. 2 and 3. This proves that the temperature at the peak shrinkage rate is decreased by increase in SiC content, as a result of the increase in amount of the intergranular liquid phase. In addition, for the same SiC content, a larger starting SiC particle size led to a lower temperature. The densities and relative densities of the resulting ZrB-based composites with SiC are summarized in Table 1. It was found that nearly fully dense ZrB_2-based composites with SiC particles were consolidated by the SPS process at 1900 °C for 3 min under a pressure of 30 MPa.

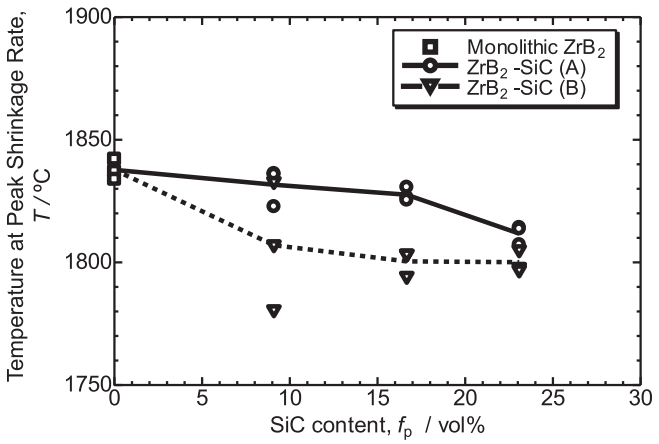

Fig. 4. Effects of SiC content on temperatures at the peak shrinkage range for ZrB_2-based composites with SiC.

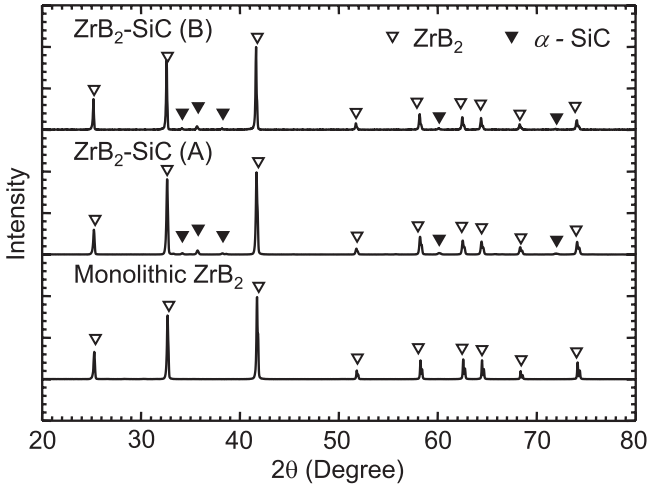

Fig. 5. X-ray diffraction patterns of ZrB_2-based composites with SiC (f_p = 23 vol.%).

It is known that improvement in densification of ZrB_2 due to addition of SiC is because of the formation of an intergranular liquid phase at the grain boundaries. Thus, the contribution to densification depended on the characteristics of the intergranular liquid phase formed because of the interactions of the compounds present in the components, including composition, content, viscosity, distribution, and wettability. According to the B_2O_3–SiO_2 phase diagram [23], the viscosity of the intergranular Si–B–O liquid phase increased with increasing SiO_2 content. In this study, the amount of SiO_2 is larger in ZrB_2–SiC(A) than in ZrB_2–SiC(B) for the same volume fraction of SiC added. Thus, the resulting intergranular liquid phase has a lower viscosity in the latter than in the former. The presence of the lower viscosity liquid phase led to a higher shrinkage rate and lower temperature at the peak shrinkage rate during the SPS cycle. However, the larger SiC particles in the ZrB_2–SiC(B) neither favored the process of grain rearrangement nor improved the packing density of particles. Conversely, the finer SiC particles in ZrB_2–SiC(A) favored grain rearrangement and enhanced the packing density of the particles. In addition, the finer SiC particles easily filled the voids left by the multiple ZrB_2 grain skeleton. The beneficial effects of the finer SiC particles on the densification were more evident during the isothermal heating (Fig. 3(a)). As a result, highly dense ZrB_2-based composites with SiC were consolidated for both composition powders in this study.

Fig. 5 shows X-ray diffraction profiles of monolithic ZrB_2 and ZrB_2-based composites with SiC consolidated by SPS. Only hexagonal ZrB_2 and hexagonal SiC were detected in every instance. This implies that no new phase formed during the SPS cycle. The microstructure of the ZrB_2-based composites with SiC was observed using SEM, typical examples of which are shown in Fig. 6. The general microstructures of the composites are similar, consisting of equiaxed ZrB_2 grains (brighter contrast) and fine and irregular SiC grains (dark contrast). The microstructure of the resulting composites is fine and homogeneous. The SiC particles were randomly dispersed in the homogeneous ZrB_2 matrix. Plots of the average grain sizes of ZrB_2 in the composite as a function of content and particle size of SiC are shown in Fig. 7. It was found that grain size decreased with increase in SiC content. This result is consistent with previous reported results in hot-pressed ZrB_2-based composites with SiC particles [6,7]. In addition, for cases with the same SiC content, fine SiC particles (SiC(A)) led to a smaller ZrB_2 grain size. This indicates that the added SiC particles inhibit grain growth of ZrB_2 during the SPS cycle. Furthermore, it was found that finer and homogeneously dispersed SiC particles in ZrB_2-based composites with SiC are more effective for inhibiting the grain growth of ZrB_2 during the SPS cycle compared with larger SiC particles.

Table 1
The compositions, densities, and relative densities of ZrB_2-based composites with SiC consolidated by spark plasma sintering.

Materials	Compositions (vol.%)		Srating particles size of SiC (μm)	Theoretical density (g/cm^3)	Measured density (g/cm^3)	Relative density (%TD)
	ZrB_2	SiC				
ZrB_2	100	0	–	6.09	5.95	97.7
ZrB_2–SiC(A)	90	10	0.5	5.80	5.76	99.3
ZrB_2–SiC(A)	80	20	0.5	5.52	5.48	99.2
ZrB_2–SiC(A)	70	30	0.5	5.23	5.21	99.7
ZrB_2–SiC(B)	90	10	6.4	5.80	5.78	99.6
ZrB_2–SiC(B)	80	20	6.4	5.52	5.46	98.9
ZrB_2–SiC(B)	70	30	6.4	5.23	5.17	98.9

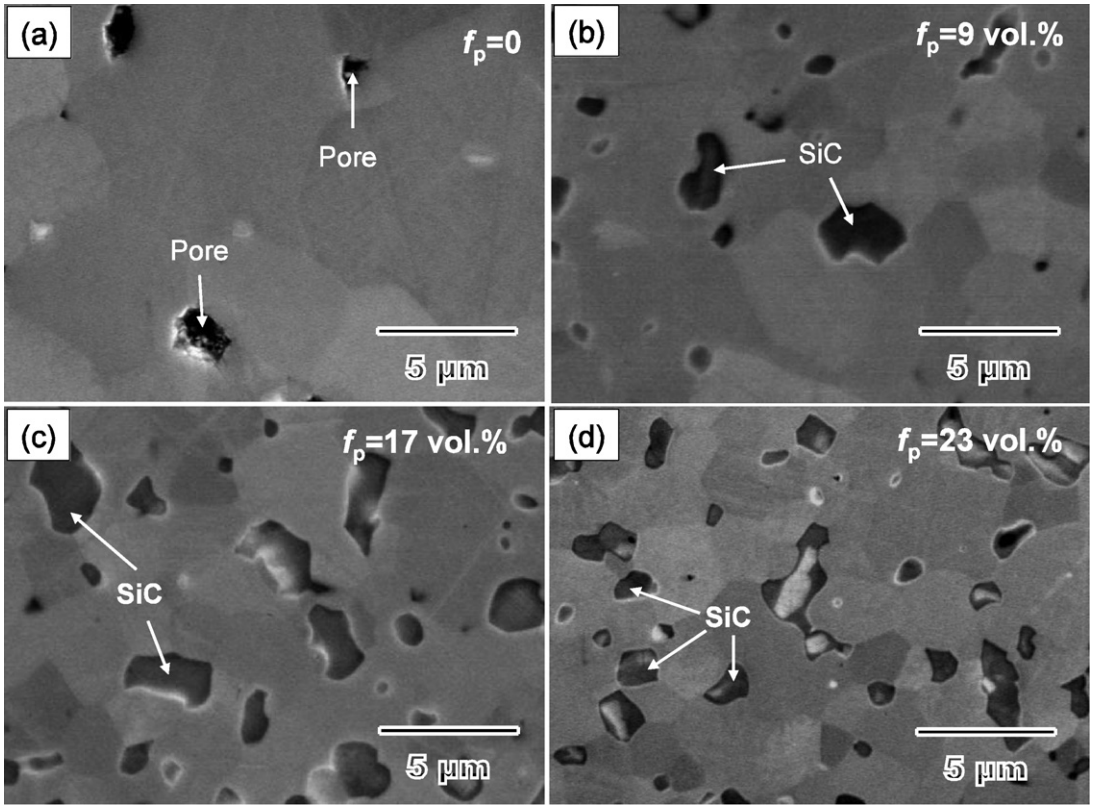

Fig. 6. Typical SEM images of ZrB_2-based composites with SiC (B).

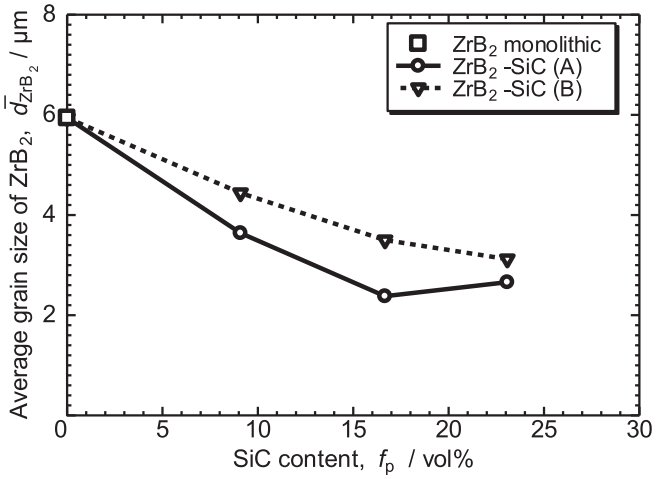

Fig. 7. Plots of average grain size of ZrB_2 as a function of SiC content for ZrB_2-based composites with SiC.

4. Summary

The densification behavior and microstructure of ZrB_2-based composites with SiC consolidated by SPS were characterized. In addition, the effects of the amount and size of the SiC particles added were examined. The following major results were obtained.

Sinterability of ZrB_2-based composites with SiC was improved, and the improvement was enhanced with increase in SiC content and decrease in particle size of the starting SiC powder. The improvement in densification is associated with increase in the shrinkage rate during the SPS cycle accompanied with the addition of SiC particles.

Nearly fully dense ZrB_2-based composites with SiC were consolidated by SPS at 1900 °C for 2 min under a pressure of 30 MPa.

The microstructure of the resulting ZrB_2-based composites with SiC was fine and homogenous. The average grain size of ZrB_2 in the composite decreases with increase in the amount of the added SiC particles, and finer SiC particles yield smaller ZrB_2 grain sizes.

Acknowledgments

The authors would like to thank Dr. T. Nishimura and Dr. H. Tanaka, National Institute for Materials Science, for preparation of composites and discussions.

References

[1] J.J.M. Martinez, A.D. Rodriguez, F. Monteverde, C. Melandri, G. Portu, Characterization and high temperature mechanical properties of zirconium boride-based materials, J. Eur. Ceram. Soc. 22 (2002) 2543–2549.
[2] M.M. Opeka, I.G. Talmy, J.A. Zaykoski, Oxidation-based materials selection for 2000 °C + hypersonic aerosurfaces: theoretical considerations and historical experience, J. Mater. Sci. 39 (2004) 5887–5904.
[3] W.G. Fahrenholtz, G.E. Hilmas, A.L. Chamberlain, J.W. Zimmermann, Processing and characterization of ZrB_2-based ultra-high temperature monolithic and fibrous monolithic ceramics, J. Mater. Sci. 39 (2004) 5951–5957.

[4] U.A. Tamburini, Y. Kodera, M. Gasch, C. Unuvar, Z.A. Munir, M. Ohyanagi, S.M. Johnson, Synthesis and characterization of dense ultra-high temperature thermal protection materials produced by field activation through spark plasma sintering (SPS): I. Hafnium Diboride, J. Mater. Sci. 41 (2006) 3097–3104.
[5] S.Q. Guo, Densification of ZrB_2-based composites and their mechanical and physical properties: a review, J. Eur. Ceram. Soc. 29 (2009) 995–1011.
[6] S.S. Hwang, A.L. Vasiliev, N.P. Padture, Improved processing and oxidation-resistance of ZrB_2 ultra-high temperature ceramics containing SiC nanodispersoids, Mater. Sci. Eng. A 464 (2007) 216–224.
[7] F. Monteverde, Beneficial effects of an ultra-fine α-SiC incorporation on the sinterability and mechanical properties of ZrB_2, Appl. Phys. A 82 (2006) 329–337.
[8] A. Bellosi, F. Monteverde, D. Sciti, Fast densification of ultra-high-temperature ceramics by spark plasma sintering, Int. J. Appl. Ceram. Technol. 3 (2006) 32–40.
[9] P. Hu, Z. Wang, Flexural strength and fracture behavior of ZrB_2-SiC ultra-high temperature ceramic composites at 1800 °C, J. Eur. Ceram. Soc. 30 (2010) 1021–1026.
[10] F. Monteverde, A. Bellosi, Beneficial effects of AlN as sintering aid on microstructure and mechanical properties of hot-pressed ZrB_2, Adv. Eng. Mater. 5 (2003) 508–512.
[11] S.C. Zhang, G.E. Hilmas, W.G. Fahrenholtz, Pressureless densification of zirconium diboride with boron carbide additions, J. Am. Ceram. Soc. 89 (2006) 1544–1550.
[12] T. Venkateswaran, B. Basu, G.B. Raju, D.Y. Kim, Densification and properties of transition metal borides-based cermets via spark plasma sintering, J. Eur. Ceram. Soc. 26 (2006) 2431–2440.
[13] S.Q. Guo, Y. Kagawa, T. Nishimura, H. Tanaka, Pressureless-sintering and physical properties of ZrB_2-based composites with $ZrSi_2$ additive, Scripta Mater. 58 (2008) 579–582.
[14] W.C. Tripp, H.C. Graham, Thermogravimetric study of oxidation of ZrB_2 in temperature range of 800 degrees to 1500 degrees, J. Electrochem. Soc. 118 (1971) 1195–1199.
[15] S.Q. Guo, Y. Kagawa, T. Nishimura, D. Chung, J.-M. Yang, Mechanical and physical behavior of spark plasma sintered ZrC-ZrB_2-SiC composites, J. Eur. Ceram. Soc. 28 (2008) 1279–1285.
[16] Z.A. Munir, U.A. Tamburini, M. Ohyanagi, The effect of electric field and pressure on the synthesis and consolidation of materials: a review of the spark plasma sintering method, J. Mater. Sci. 41 (2006) 763–777.
[17] T. Nishimura, M. Mitomo, H. Hirotsuru, M. Kawahara, Fabrication of silicon nitride nano-ceramics by spark plasma sintering, J. Mater. Sci. Lett. 14 (1995) 1046–1047.
[18] S.Q. Guo, T. Nishimura, Y. Kagawa, J.-M. Yang, Spark plasma sintering of zirconium diborides, J. Am. Ceram. Soc. 91 (2008) 2848–2855.
[19] S.Q. Guo, J.-M. Yang, H. Tanaka, Y. Kagawa, Effect of thermal exposure on strength of ZrB_2-based composites with nano-sized SiC particles, Compos. Sci. Technol. 68 (2008) 3033–3040.
[20] M. Pastor, Metallic borides: preparation of solid bodies. Sintering methods and properties of solid bodies, in: V.I. Matkovich (Ed.), Boron and Refractory Borides, Springer, New York, 1977, pp. 457–493.
[21] R. Telle, L.S. Sigl, K. Takagi, Boride-based hard materials, in: R. Riedel (Ed.), Handbook of Ceramic Hard Materials, 2, Wiley-VCH, Weinheim, Germany, 2000, pp. 802–945.
[22] S. Baik, P.F. Becher, Effect of oxygen contamination on densification of TiB_2, J. Am. Ceram. Soc. 70 (1987) 527–530.
[23] T.J. Rockett, W.R. Foster, Phase relations in the system boron oxide-silica, J. Am. Ceram. Soc. 48 (1965) 75–80.